environments

MDPI

Article

Evaluating the Efficacy of Thiolating Agents for Biochar Surface Modification

Oluyinka Aduloju [1], Arnav Pandey [1], Frieda Eivazi [2], Sougata Bardhan [2] and Zahra Afrasiabi [1,2,*]

[1] Life Sciences, Soka University of America, Aliso Viejo, CA 92656, USA
[2] Department of Agriculture & Environmental Sciences, Lincoln University, Jefferson City, MO 65101, USA
* Correspondence: zafrasiabi@soka.edu

Abstract: As a cost-effective sorbent, modified biochar has received increasing attention for the removal of heavy metal contaminants. Among several chemical modification methods, introducing thiol functional groups onto the surface of biochar has been identified as an effective enhancement approach for the heavy metal sorption and removal capacity of this porous adsorbent material. In general, chemical impregnation is a widely used method to graft thiol groups onto the surface of carbon-based materials. However, limited comparative data are available on the efficacy of the present biochar thiolation methods. In this study, the biochar of nine different organic sources was modified by two frequently used agents with distinct thiolation mechanisms: 3-Mercaptopropyltrimethoxysilane (3-MPTS) and β-mercaptoethanol. In addition to chemical impregnation, the ball milling method, a simple and environmentally friendly alternative thiolation method, was also evaluated. A comprehensive structural characterization of the biochar samples was completed before and after thiolation. A higher concentration of sulfur on the surface of the biochar was achieved through thiolation with β-mercaptoethanol, in which the thiolation mechanism is performed through an esterification reaction with the carboxylic acid functional groups of the activated biochar. Chemical impregnation was found to be a more effective thiolating method than ball milling using the same thiolating agent.

Keywords: thiol modification; 3-MPTS; β-mercaptoethanol

check for updates

Academic Editor: Nelson Belzile

Received: 13 January 2025
Revised: 25 February 2025
Accepted: 1 March 2025
Published: 11 March 2025

Citation: Aduloju, O.; Pandey, A.; Eivazi, F.; Bardhan, S.; Afrasiabi, Z. Evaluating the Efficacy of Thiolating Agents for Biochar Surface Modification. *Environments* **2025**, *12*, 84. https://doi.org/10.3390/environments12030084

Copyright: © 2025 by the authors. Licensee MDPI, Basel, Switzerland. This article is an open access article distributed under the terms and conditions of the Creative Commons Attribution (CC BY) license (https://creativecommons.org/licenses/by/4.0/).

1. Introduction

Biochar is an organic, porous, carbon-rich material produced by the pyrolysis of a wide range of organic biomass, like agricultural residue, manure, and wood, in the absence or with a limited supply of oxygen [1–4]. Besides carbon, biochar contains nitrogen, hydrogen, oxygen, and macronutrients essential for soil, such as silicon, phosphorus, sulfur, and iron, in varying amounts depending on the biomass source [5]. Since the raw materials to make biochar are easily available in the surrounding environment and the procedure to make it is undemanding, recent studies have reported on biochar as a simple, low-cost, and highly efficient adsorbent for environmental pollution remediation through the chemical immobilization of heavy metals like cadmium (II), copper (II), lead (II), nickel (II), and zinc (II) in the soil [6–11]. The amendment of biochar, which contains different negatively charged functional groups on the surface, into the soil as a chemical immobilizing agent lowers the mobility and bioavailability of heavy metals through ion exchange, adsorption, complexation, and precipitation reactions [12]. However, for practical remediation applications, biochar suffers from low selectivity, a low capacity, and a weak binding affinity for heavy metals [13]. Therefore, a number of modification methods have been developed

to optimize biochar's remediation efficiency, including surface mineral and nanoparticle doping [14–19], changes in the surface functional groups by acid/base activation [20,21], hydrogen peroxide treatment [22], chitosan coating [23], and thiol modification [24,25].

Due to the high affinity of thiol groups for heavy metal ions, grafting thiol functional groups onto the surface of biochar has been repeatedly reported to improve biochar's adsorption capacity and selectivity toward heavy metal ions [26–29]. Surface thiol modification introduces more negative charges onto the biochar and enhances the electrostatic adsorption of positively charged contaminants, such as heavy metal ions. The sorption of heavy metals on biochar adsorption sites is enhanced by ligand exchange, complexation, and a soft Lewis acid-base interaction [30].

A widely used thiol functionalization agent is 3-Mercaptopropyltrimethoxysilane (3-MPTS). After hydrolyzation under certain conditions, it can dehydrate or engage in ligand exchange with hydroxyl groups on the surface of biochar. In addition, it can form a strong interfacial adhesion with oxygen-containing groups (e.g., hydroxyl, carboxyl, and carbonyl) and graft thiol groups onto the surface [31–33]. β-mercaptoethanol is another reagent used by researchers to introduce thiol groups onto the carbon surfaces treated by strong acidic oxidants. In this process, thiol functionalization takes place through an esterification reaction between the hydroxyl group of the reagent and the carboxylic group on the activated biochar surface [24,34].

The specific objective of this study was to comparatively evaluate the thiolation efficiency of two widely used thiolating agents (i.e., 3-MPTS and β-mercaptoethanol) on biochar samples. In addition to these chemical impregnation methods, ball milling was investigated to determine if this environmentally friendly method could be utilized as a viable alternative experimental procedure for biochar thiol modification. The structure and physicochemical properties of the modified biochar were studied.

2. Material and Methods

2.1. Materials

All chemicals used in this study were of analytical grade or higher and were purchased from Sigma Aldrich (St. Louis, MO, USA). The following chemicals were used in the experimental procedures: ethanol (200 proof, anhydrous, ≥99.5%), 3-(mercaptopropyl) trimethoxysilane (95%), ammonium hydroxide (29% NH_3 in H_2O), β-mercaptoethanol (99%), acetic anhydride (99%), and concentrated sulfuric acid. All reagents were used as received, without further purification. Ultrapure water (Millipore, 18.2 MΩ·cm, Merck KGaA, Darmstadt, Germany) was used to prepare all solutions. Feedstock for the preparation of the pristine biochar samples was collected from different organic sources (Jefferson City, MO, USA), including corncob (B1), wheat chaff (B2), sweet gum (B3), sunflower heads (B4), eastern red cedar (B5), bush honeysuckle (B6), mixed hardwood (B7), pinecone (B8), and Christmas fir tree (B9).

2.2. Instrumentation

The carbon, nitrogen, and sulfur contents were determined using a Thermo Scientific™ FlashSmart™ 2000 elemental analyzer (Waltham, MA, USA). Vanadium pentoxide was added to aid in complete combustion. Vertical Lab Planetary Ball Mill DECO-V400ML from UBE Nanotechnology (China) was used for ball milling. Fourier transform infrared (FT-IR) (Perkin Elmer UATR Two, Bucks, UK) analysis was applied to analyze the surface functional groups over a range of 400–4000 cm^{-1}, with a 1 cm^{-1} resolution. A Thermo Scientific™ VolumeScope™ scanning electron microscope (SEM) (Waltham, MA, USA) was used to characterize the structure and surface morphology of the pristine and thiolated biochar samples. The samples were dispersed onto a C adhesive and sputter-coated with

10 nm Pt to improve the image quality. The images were collected at 5 kV using secondary electrons. To measure the zeta potential of the pristine and thiolated biochar, the samples were ground and passed through a 60-mesh sieve. Then, 5 mg of each sample in 25 mL of 0.001 M KCl solution was ultrasonically dispersed in a bath-type sonicator at a frequency of 40 kHz and a power of 300 W for 2 h at 25 °C. All solutions were in the neutral pH range. After sonication, the suspensions were allowed to stand for 1 d, and the zeta potential values were measured using a Malvern Nano Zetasizer (Worcestershire, UK). The surface atomic ratio (C, N, O, S, and Si) and binding energy of C1s, N1s, S2p, and Si2p were analyzed by X-ray photoelectron spectroscopy (XPS) using a Thermo Scientific™ NEXSA™ surface analysis system with an Al K-α X-ray source adjustable in the range of 10–100 mm (hv = 1486.6 eV) and an EX06 monatomic ion source (200 eV–4 keV ion energy). The energy step size was 0.1 eV for each element scan and 0.5 eV for a wide scan. XPS spectra were analyzed using CasaXPS software (version 2.3.25) with Gaussian–Lorentzian line shapes having 30% Lorentzian character, GL (30) [35]. Atomic concentration calculations from the survey scans were performed using Scofield cross-sections.

2.3. Preparation of Pristine and Thiolated Biochar

The nine pristine biochar samples were obtained by air drying and carbonizing each sample at 500 °C in an oxygen-limited condition for about 3 h. The solid samples were pounded into a powdery form using a mortar and pestle, passed through a 60-mesh sieve (CD1-1KT, Sigma Aldrich, MO, USA), and thiolated using three thiolation methods: chemical impregnation with the 3-MPTS reagent [36], ball milling with the 3-MPTS reagent [31], and chemical impregnation with β-mercaptoethanol [24]. The experimental procedure for each method is described below.

2.3.1. Chemical Impregnation with the 3-MPTS Reagent (BX-3M Thiolated Biochar Sample Series)

First, 3 g of biochar was mixed with 3.6 mL of ultrapure water (DI) and 114 mL of ethanol; 2.4 mL of 3-MPTS was added using a syringe pump at a 10 mL/min flow rate. After stirring the mixture under nitrogen flow for 6 h, the pH was adjusted by adding an NH_4OH solution. The reaction was stopped after 24 h, and the modified biochar was filtered using VWR grade 413 papers under vacuum conditions and washed with water and ethanol. To ensure the removal of the unreacted 3-MPTS, the washing process was repeated three times.

2.3.2. Ball Milling with the 3-MPTS Reagent (BX-BA Thiolated Biochar Sample Series)

In a 100 mL agate jar, 60 g of agate balls were weighed out with proportions of 12 g of 15 mm, 30 g of 5 mm, and 18 g of 3 mm. Subsequently, 0.6 g of biochar, 0.72 mL of DI water, 22.8 mL of ethanol, and 0.48 mL of 3-MPTS were added to the agate jar. The jar was set to 300 rpm for 12 h, and the rotation direction was changed after 6 h. After the time elapsed, the reaction mixture was filtered.

2.3.3. Chemical Impregnation with β-Mercaptoethanol Reagent (BX-BM Thiolated Biochar Sample Series)

Initially, 1 g of biochar and 4 mL of β-mercaptoethanol were mixed in a 10 mL brown glass bottle. Next, 2.8 mL of acetic anhydride followed by 0.2 mL of concentrated H_2SO_4, were added to the stirring mixture dropwise. The reaction container was closed, and the mixture was heated in an oil bath at 80 °C and set on a shaker. After 18 h, the reaction was stopped, and the modified biochar was filtered.

The products of all three experiments were dried in a vacuum oven at room temperature and 16 mm Hg for 48 h, and the dried samples were sieved with a 60-mesh sieve.

3. Results and Discussion

The two reagents used in this study have distinct reaction mechanisms for grafting thiol groups onto the biochar's surface. The methoxy group on the 3-MPTS hydrolyzes and desorbs as methanol. The remaining structural part either on its own or after going through self-polymerization can dehydrate or engage in ligand exchange with hydroxyl groups on the surface of the biochar, forming a strong interfacial adhesion or becoming involved in a π-π interaction with other oxygen-containing functional groups on the surface of the biochar [37,38]. Researchers found that 3-MPTS introduced the most –SH groups and resulted in the highest negative charge in carbon-based material when impregnation took place in ammonium hydroxide rather than in an acidic or neutral medium [37]. Therefore, in this study, thiol chemical impregnation was carried out in the basic medium. However, the thiol functionalization of biochar by β-mercaptoethanol is essentially a two-step process. Initially, the treatment of biochar with the oxidant sulfuric acid increases the surface carboxyl group distribution. β-mercaptoethanol has a thiol group at one end of the molecule and an –OH group at the other. Next, the esterification reaction between the carboxyl-activated biochar and the hydroxyl group of the reagent adds thiol groups onto the surface of the biochar [39]. All nine biochar samples in this study were structurally characterized prior to and after thiolation.

The elemental analysis clearly indicated a change in the composition of the biochar samples after thiol modification (Table S1), with an increase in the sulfur content in all of the modified biochar. The β-mercaptoethanol reagent introduced the highest concentration of sulfur (S%: 26–33% in BX-BM) compared to the samples that reacted with the 3-MPTS reagent (S%: 1–4% in BX-BA and 4–7% in BX-3M).

To identify the chemical changes in the functional groups on the biochar's surface, the FT-IR spectra of the thiolated and pristine biochar samples were obtained (Figure 1). Significant differences were found when comparing the spectra of the pristine biochar to the thiolated biochar in all three methods (Table S2). The pristine biochar showed peaks at 1554–1582 cm^{-1}, 1366–1411 cm^{-1}, 1023–1175 cm^{-1}, 610–624 cm^{-1}, and 454–484 cm^{-1}, which correspond to the C=C, C–OH, C–O carboxylic, C–O alkyl, and C–C bonds [40].

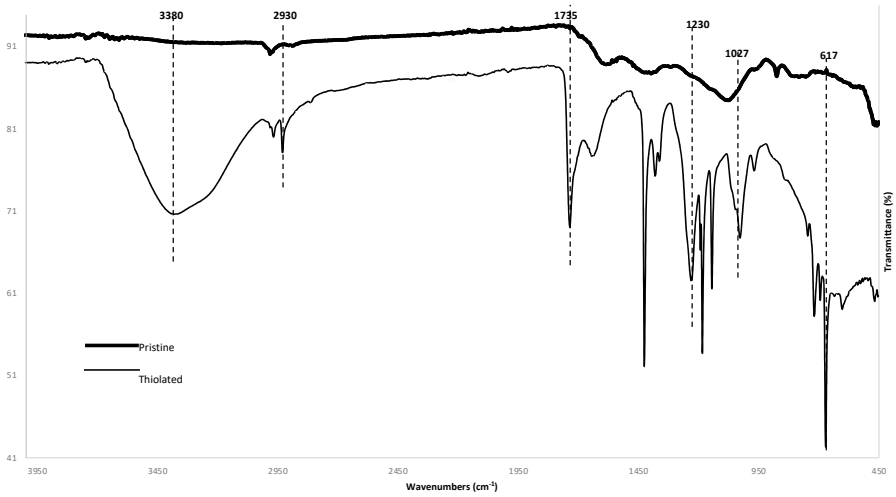
Using the β-mercaptoethanol method, the peaks at 2930–2931 cm^{-1} and 1734–1736 cm^{-1} were attributed to the O–CH_2 vibrations of β-mercaptoethanol and to C=O ester carbonyl stretching, respectively [24,41]. These results show that the thiol group was grafted to the biochar surface through ester linkages [42]. The peaks at 671–672 cm^{-1} were assigned to the carbon–sulfur vibration, thus confirming the presence of β-mercaptoethanol in the thiolated biochar [27]. Signals at 1228–1231 cm^{-1} and 1027–1028 cm^{-1} were attributed to lactones and to the stretching vibration of C–O [24,43].

The vibration band at 1040 cm^{-1} (attributed to S=O symmetric stretching), which would indicate the presence of sulfonic groups (–SO_3H), was not visible in the FT-IR spectra of the BX-BM samples. Additionally, the absence of this vibration band indicates that sulfonic groups were not formed during the thiol modification of the pristine biochar even though concentrated H_2SO_4 was added to the reaction during preparation [44]. Therefore, β-mercaptoethanol was successfully introduced onto the pristine biochar by esterification [45].

Samples thiolated using 3-MPTS and ammonium hydroxide reagents (BX-3M) showed peaks at 1024–1033 cm^{-1}, 1566–1747 cm^{-1}, and 1391–1396 cm^{-1}, which correspond to the signals present in the pristine biochar but with a reduced intensity that might be attributable to the stretching vibrations of the broad –OH peak at 3215–3339 cm^{-1} [46–48]. These changes suggest that oxygen-containing functional groups (i.e., –OH and C–O) and a π–π bond played a significant role in the 3-MPTS linking to the surface of the biochar. The results also show new peaks at 686–689 cm^{-1}, suggesting the presence of a C–S bond,

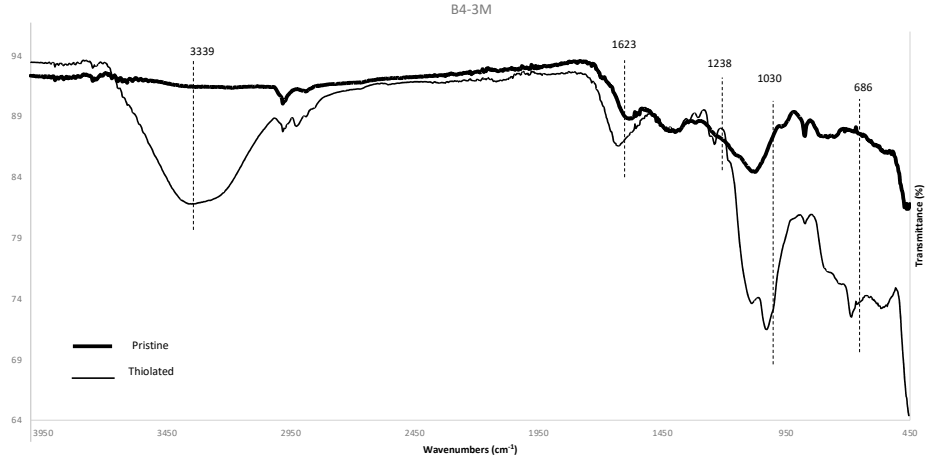
evidence that 3-MPTS was attached to the surface of the pristine biochar successfully using this method.

Chemical impregnation with β-mercaptoethanol reagent (B4–BM).



B4-BM

Chemical impregnation with the 3-MPTS reagent (B4–3M).



Ball milling with the 3-MPTS reagent (B4–BA).

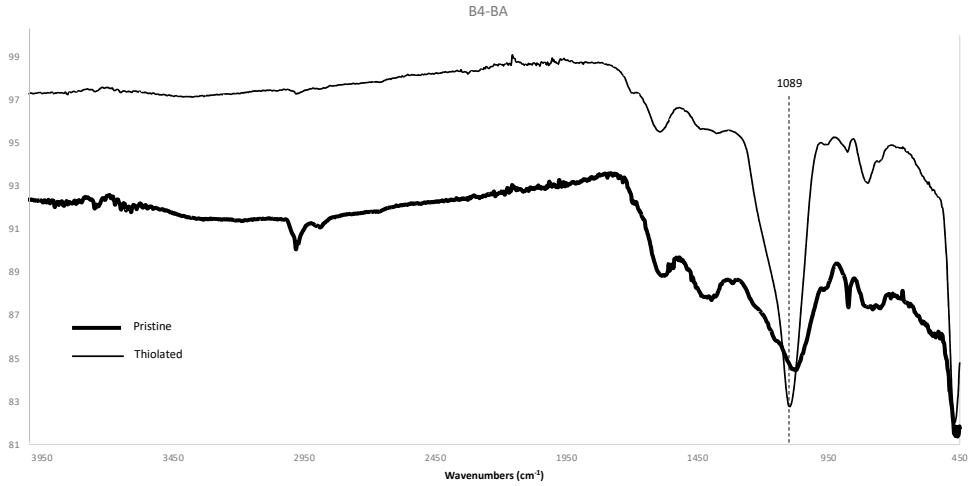


Figure 1. FTIR spectra of pristine and thiolated biochar of sample 4 using three thiolation methods.

The spectra of the biochar modified by the ball milling method showed peaks at 1459–1591 cm^{-1} and 1042–1099 cm^{-1}, which correspond to the C=C and C–O bonds. New

peaks were observed at 747–799 cm^{-1} and 874–881 cm^{-1}, which signify the presence of C–S and Si–O bonds, respectively [26]. Although the presence of C–S bonds indicates that the thiol functional group was added successfully, the peaks only occurred in a few samples, suggesting that the ball milling method was not as efficient and effective as the other two methods in adding thiol groups to the pristine biochar.

The particle morphology of the pristine and thiolated biochar was compared using scanning electron microscopy (SEM) images. During the process of sputtering the samples for the SEM analysis, a considerable amount of charging was noticed in all thiolated biochar compared to the pristine biochar. The broad overview of the particle sizes in Figure 2 and Figure S1 shows a higher degree of aggregation in the BX-3M samples compared to the other two thiolated samples. This might be the result of introducing more hydrophilic groups onto the surface of the biochar, resulting in enhanced hydrophilicity, which could have facilitated the formation of aggregates [49]. With higher magnification, as presented in Figure 3 and Figure S2, the rough, porous, and regular polygon structure of the pristine biochar was clearly observed in all samples. BX-3M thiolated biochar retained a similar morphology to a great extent, except that the surface became slightly smoother. This could be the result of exposure to solvents and coating with the 3-MPTS reagent during the thiolation process. On the other hand, in the BX-BA samples, ball milling with the same thiolating reagent completely broke the biochar particles into nanosized fine grains with an amorphous structure [50].

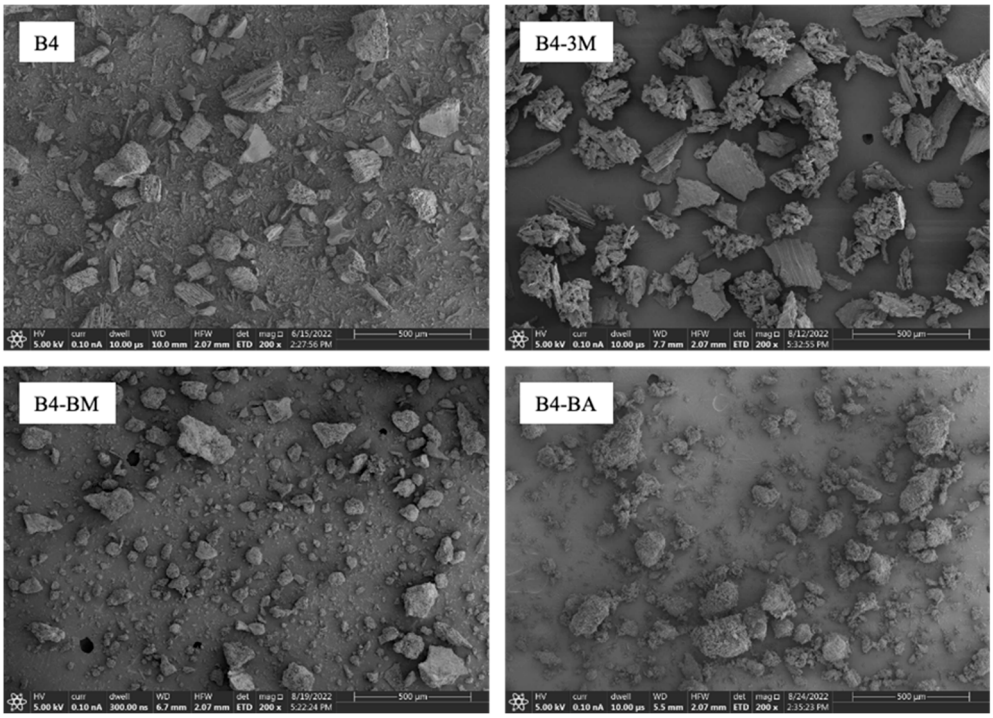


Figure 2. SEM images of pristine biochar (B4), thiolated biochar using β-mercaptoethanol (B4-BM), thiolated biochar with 3-MPTS (B4-3M), and thiolated biochar with 3-MPTS using a ball mill (B4-BA) at a 500 mm scale.

All pristine biochar samples showed a negative zeta potential in the range of –19 to –48 mV, which was mainly due to the presence of negatively charged oxygen-containing functional groups on the colloidal particle surfaces (Table 1) [51,52]. During thiol modification with 3-MPTS (BX-3M and BX-BA samples), some oxygen-containing functional groups reacted and combined with the 3-MPTS reagent. The resulting thiolated biochar showed more negative zeta potential, which indicates that the negative charges introduced

as a result of the 3-MPTS hydrolysis compensated for the negative charges lost. In contrast, thiolation with β-mercaptoethanol substantially increased the zeta potential of the biochar surfaces. Although some of the surface of the BX-BM samples held negative charges resulting from a higher thiolation rate of the β-mercaptoethanol, the esterification reaction between the hydroxyl group of the reagent and the biochar carboxyl group reduced the availability of these negative charges on the surface.

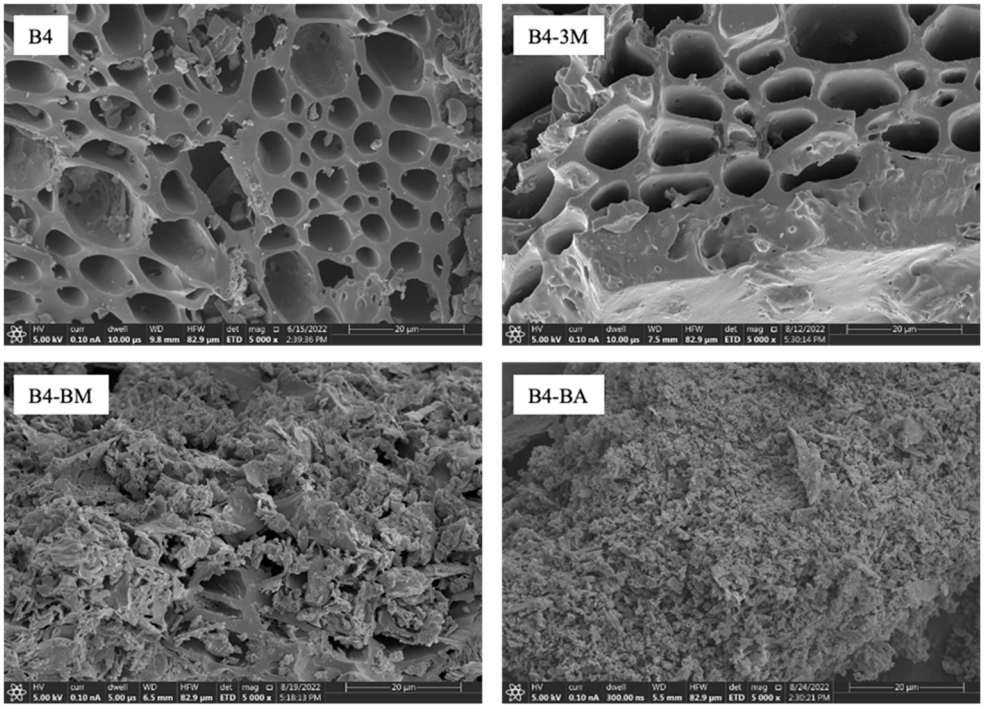


Figure 3. SEM images of pristine biochar (B4), thiolated biochar using β-mercaptoethanol (B4-BM), thiolated biochar with 3-MPTS (B4-3M), and thiolated biochar with 3-MPTS using a ball mill (B4-BA) at a 20 mm scale.

Table 1. The zeta potential values (mV) of pristine biochar (BX), thiolated biochar using β-mercaptoethanol (BX-BM), thiolated biochar with 3-MPTS (BX-3M), and thiolated biochar with 3-MPTS using a ball mill (BX-BA) in a 0.001 M KCl solution.

	B1	**B2**	**B3**	**B4**	**B5**	**B6**	**B7**	**B8**	**B9**
Pristine	−26.01 ± 1.19	−23.37 ± 0.56	−26.00 ± 4.55	−48.45 ± 1.92	−24.48 ± 1.99	−18.78 ± 1.86	−31.78 ± 1.59	−43.03 ± 1.67	−40.97 ± 1.81
BX-3M	−47.7 ± 1.45	−43.08 ± 2.64	−33.33 ± 4.06	−50.45 ± 2.13	−40.62 ± 2.30	−51.38 ± 2.80	−52.37 ± 1.95	−35.68 ± 2.33	−49.27 ± 1.67
BX-BM	−1.91 ± 1.11	−4.56 ± 2.25	−2.21 ± 1.76	−2.43 ± 2.19	−3.23 ± 3.24	−4.78 ± 0.44	−0.52 ± 1.96	−0.82 ± 1.17	1.72 ± 1.15
BX-BA	−43.68 ± 4.59	−44.78 ± 1.68	−47.23 ± 2.16	−45.00 ± 1.61	−46.13 ± 2.11	−48.87 ± 1.87	−38.93 ± 1.18	−48.55 ± 1.60	−44.95 ± 2.01

The wide-scan XPS spectra of the pristine and thiolated biochar are shown in Figure 4 and Figure S3, in which C 1s, O 1s, N 1s, S 2p, and Si 2p peaks can be observed. The relative surface concentration of the elements identified by the XPS spectra are listed in Table S3. S 2s was used for quantification to avoid the overlap of S 2p with the structure loss of Si2s.

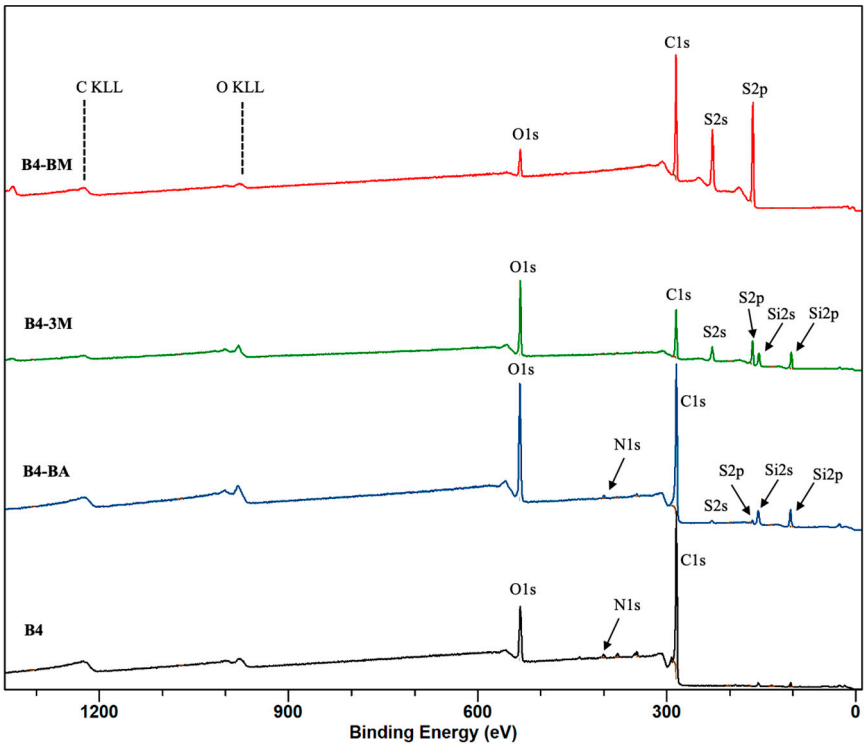


Figure 4. XPS wide scan of pristine biochar (B4), thiolated biochar using β-mercaptoethanol (B4-BM), thiolated biochar with 3-MPTS (B4-3M), and thiolated biochar with 3-MPTS using a ball mill (B4-BA).

As presented in Figure 5 and Figure S4, the four fitted components in the C 1s peak area are attributed to C–C/C=C/C–H (283.9–284.8 eV), C–O (285.3–286.3 eV), C=O (286.7–287.7 eV), and O–C=O (287.8–288.8 eV) bonds [33,53]. The relative proportions of each component are presented in Table S4. After thiolation with 3-MPTS, the % C–C, C=C, and C–H increased, but the % C–O, C=O, and O–C=O decreased in all samples (BX-3M). This indicates that the 3-MPTS coated the surface of the biochar samples predominantly through oxygen-containing functional groups (i.e., C–O, C=O, and O–C=O). The opposite was observed when ball milling was used with the same thiolating reagent in the BX-BA samples. Similarly, in the β-mercaptoethanol-modified samples (BX-BM), a decrease in C=O intensity was observed in all of the thiolated samples. For samples B1, B2, B3, B7, and B9, the C–O intensity increased, while the C–C/C=C/C–H intensities decreased; this signifies that some part of the coating could result from a C=C p-p interaction [37]. Modification with 3-MPTS (BX-3M) produced the highest concentration ratios of O/C and O+N/C in all samples, with an observed order of BX-3M > BX-BA > BX-BM > BX. This could be an indication of the presence of more O-containing functional groups on the surface, and subsequently, a more hydrophilic surface.

The thiolated biochar samples appeared to have more surface charges that resulted in broadening the XPS peaks. Two sets of doublets were used for the S 2p peaks to propagate the curve fitting to all spectra (Table S5). The S 2p binding energies in the thiolated biochar at 162.5–163.2 eV were ascribed to S 2p (–SH) and C–S/S=S, which have very similar binding energies and are therefore not distinguishable (Figure 6 and Figure S5) [54]. Overall, the S concentration was extremely low for the pristine biochar (0–0.3%), which is evident from the weak S 2s and S 2p peaks. The maximum sulfur concentration was observed in β-mercaptoethanol-thiolated samples (BX-BM, 24–32% S). Less thiolation was observed when the 3-MPTS reagent was used (BX-3M, 9–14% S). The ball milling biochar samples with 3-MPTS showed the least sulfur concentration (BX-BA, 0–7% S) compared to the samples that were stirred under nitrogen with the same reagent.

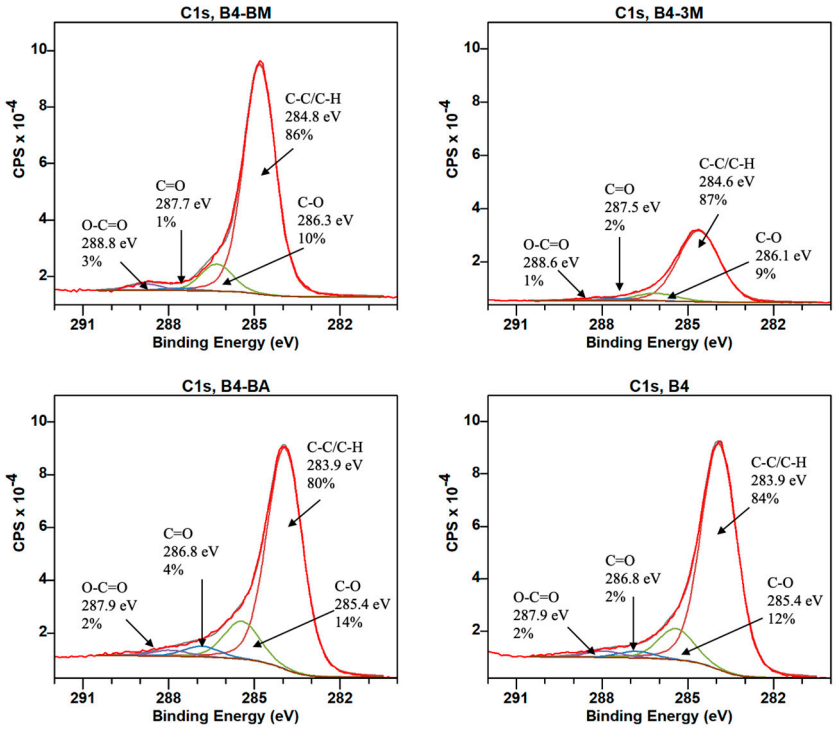


Figure 5. XPS spectra of C 1s for pristine biochar (B4), thiolated biochar using β-mercaptoethanol (B4–BM), thiolated biochar with 3-MPTS (B4–3M), and thiolated biochar with 3-MPTS using a ball mill (B4–BA).

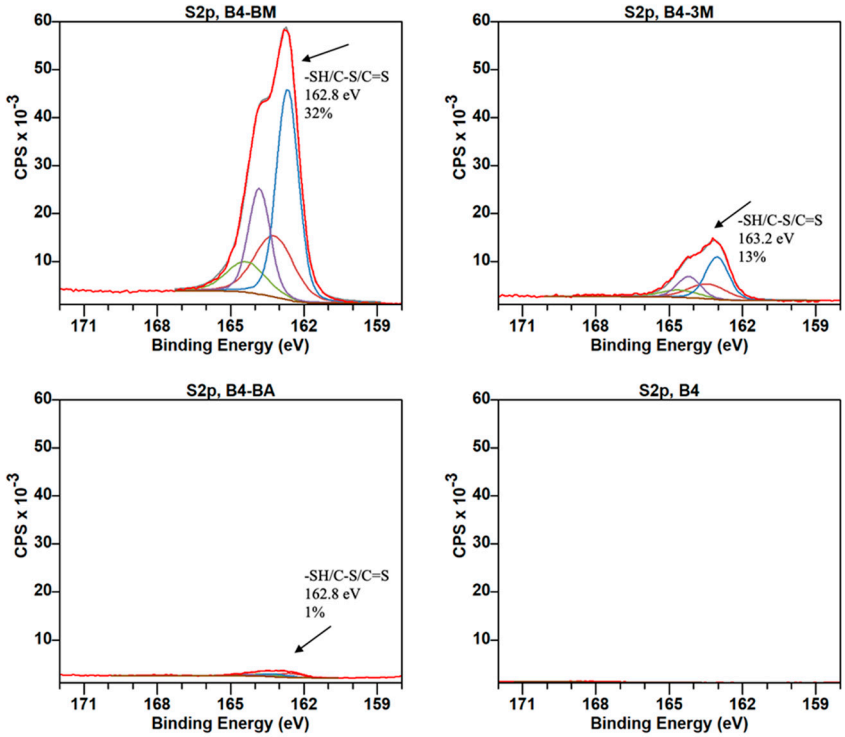


Figure 6. XPS spectra of S 2p for pristine biochar (B4), thiolated biochar using β-mercaptoethanol (B4–BM), thiolated biochar with 3-MPTS (B4–3M), and thiolated biochar with 3-MPTS using a ball mill (B4–BA).

Si peaks at 101.2–102.92 eV attributed to Si°, Si–C, Si–O, and SiO_2 were observed in the biochar samples thiolated with 3-MPTS, with a higher Si concentration observed in the BX-3M biochar (12–17% Si) compared to the ball milled samples (BX-BA; 1–9% Si),

as depicted in Figure 7 and Figure S6 [36,55]. As expected, since the β-mercaptoethanol reagent did not contain silicon, the thiolation of the biochar samples with this reagent did not increase the Si content in the BX-BM products.

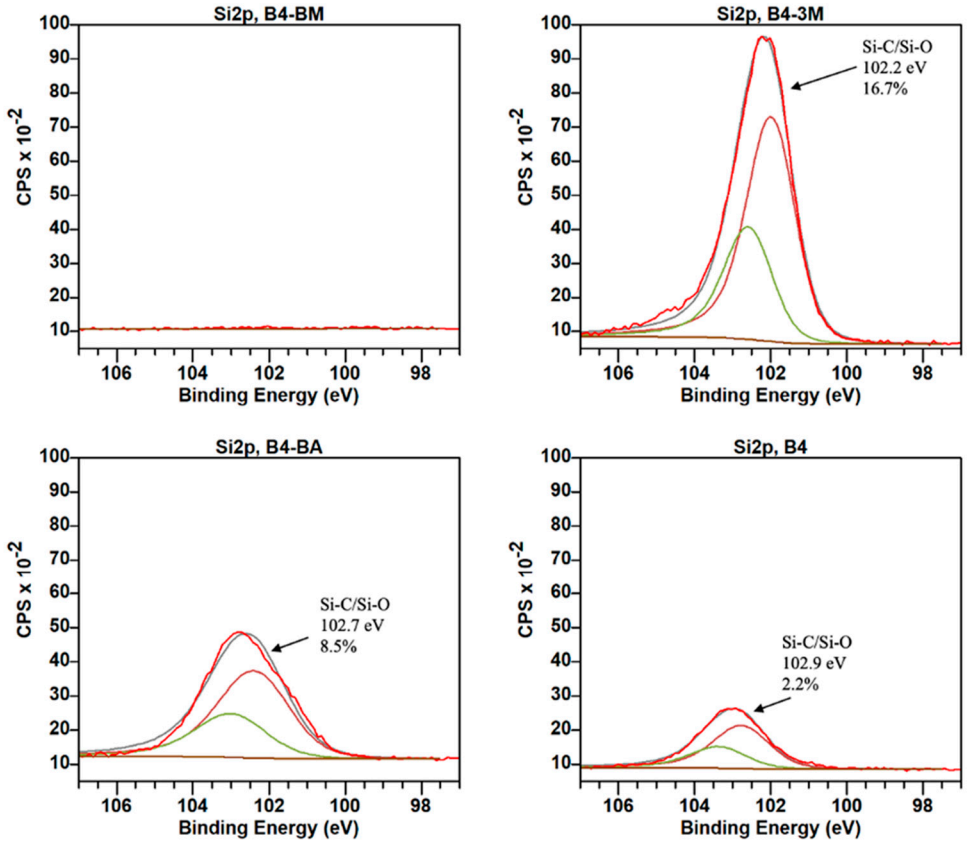


Figure 7. XPS spectra of Si 2p for pristine biochar (B4), thiolated biochar using β-mercaptoethanol (B4–BM), thiolated biochar with 3-MPTS (B4–3M), and thiolated biochar with 3-MPTS using a ball mill (B4–BA).

4. Conclusions

In this study, the organic source of the biochar had a negligible effect on the extent of thiolation using the three methods. The highest concentration of thiolation was achieved when applying the β-mercaptoethanol reagent. Although the simple and environmentally friendly method of ball milling can usually break chemical bonds, increase the specific surface area, and create new surfaces, in our study, the ball milling method conducted using the reported optimized experimental condition was not as effective in attaching sulfur groups to the biochar as the chemical impregnation method using the same reagent [31,56]. Further experimentation is needed to investigate the effect of the biochar-to-ball mass ratio, ball milling time, and rotation speed. Researchers have been thiolating biochar to improve the heavy metal adsorption capacity and selectivity, and our analysis revealed that, by far, the reagent β-mercaptoethanol has better efficacy in loading thiol groups onto biochar compared to the 3-MPTS reagent. However, electrostatic attraction, ligand exchange, and surface complexation through active sites other than thiol groups (i.e., oxygen-containing functional groups) have also been reported as possible removal mechanisms for metal ions. Our characterization results reveal that thiol modification through 3-MPTS chemical impregnation introduces more negative charges onto the biochar's surface relative to the products of the other two applied methods. Hence, for the removal of metal ions, having an insight into the sorption mechanism can be a key factor in choosing the optimal thiolating reagent, and the amount of introduced sulfur should not be the only consideration.

Supplementary Materials: The following supporting information can be downloaded at: https://www.mdpi.com/article/10.3390/environments12030084/s1, Figure S1: The SEM images of pristine biochar (BX), thiolated biochar using b-mercaptoethanol (BX-BM), thiolated biochar with 3-MPTS (BX-3M), and thiolated biochar with 3-MPTS using a ball-mill (BX-BA) at 500 mm scale; Figure S2: The SEM images of pristine biochar (BX), thiolated biochar using b-mercaptoethanol (BX-BM), thiolated biochar with 3-MPTS (BX-3M), and thiolated biochar with 3-MPTS using a ball-mill (BX-BA) at 20 mm scale; Figure S3: The XPS wide scan of pristine biochar (BX), thiolated biochar using b-mercaptoethanol (BX-BM), thiolated biochar with 3-MPTS (BX-3M), and thiolated biochar with 3-MPTS using a ball-mill (BX-BA); Figure S4. XPS spectra of C1s for pristine biochar (BX), thiolated biochar using b-mercaptoethanol (BX-BM), thiolated biochar with 3-MPTS (BX-3M), and thiolated biochar with 3-MPTS using a ball-mill (BX-BA); Figure S5. XPS spectra of S 2p for pristine biochar (BX), thiolated biochar using b-mercaptoethanol (BX-BM), thiolated biochar with 3-MPTS (BX-3M), and thiolated biochar with 3-MPTS using a ball-mill (BX-BA); Figure S6. XPS spectra of Si 2p for pristine biochar (BX), thiolated biochar using b-mercaptoethanol (BX-BM), thiolated biochar with 3-MPTS (BX-3M), and thiolated biochar with 3-MPTS using a ball-mill (BX-BA); Table S1: CHNS elemental analysis result for pristine and thiolated biochar; Table S2: FTIR analysis of pristine and thiolated biochar; Table S3: Relative surface concentration of identified elements for pristine biochar (BX), thiolated biochar using b-mercaptoethanol (BX-BM), thiolated biochar with 3-MPTS (BX-3M), and thiolated biochar with 3-MPTS using a ball-mill (BX-BA); Table S4. Peak fitting results of XPS C1s peaks for pristine and thiolated biochar samples; Table S5. Peak fitting results of XPS S 2p peaks for pristine and thiolated biochar samples.

Author Contributions: Conceptualization, Z.A.; methodology, O.A., A.P. and Z.A.; software, O.A., A.P. and Z.A.; validation, O.A., A.P. and Z.A.; formal analysis, O.A., A.P. and Z.A.; investigation, O.A., A.P. and Z.A.; resources, F.E., S.B. and Z.A.; data curation, O.A., A.P. and Z.A.; writing—original draft preparation, O.A., A.P. and Z.A.; writing—review and editing, O.A., A.P. and Z.A.; visualization, O.A., A.P. and Z.A.; supervision, Z.A.; project administration, Z.A.; funding acquisition, F.E., S.B. and Z.A. All authors have read and agreed to the published version of the manuscript.

Funding: This study was funded by the Stauffer Charitable Trust, Soka University of America's Presidential Research Assistantship, and the United States Department of Agriculture (USDA) grant number [2022-51300-37883].

Data Availability Statement: The original contributions presented in this study are included in the article/Supplementary Materials. Further inquiries can be directed to the corresponding author.

Conflicts of Interest: The authors declare no conflict of interest.

References

1. Isaac, D.; Labbancz, J.; Knowles, N.R.; Tenic, E.; Horgan, A.; Ghogare, R.; Dhingra, A. Biomass Source of Biochar and Genetic Background of Tomato Influence Plant Growth and Development and Fruit Quality. *Horticulturae* **2024**, *10*, 368. [CrossRef]
2. Khan, S.; Irshad, S.; Mehmood, K.; Hasnain, Z.; Nawaz, M.; Rais, A.; Gul, S.; Wahid, M.A.; Hashem, A.; Abd_Allah, E.F.; et al. Biochar Production and Characteristics, Its Impacts on Soil Health, Crop Production, and Yield Enhancement: A Review. *Plants* **2024**, *13*, 166. [CrossRef] [PubMed]
3. Rajput, V.; Saini, I.; Parmar, S.; Pundir, V.; Kumar, V.; Kumar, V.; Naik, B.; Rustagi, S. Biochar Production Methods and Their Transformative Potential for Environmental Remediation. *Discov. Appl. Sci.* **2024**, *6*, 408. [CrossRef]
4. Zhou, Y.; Qin, S.; Verma, S.; Sar, T.; Sarsaiya, S.; Ravindran, B.; Liu, T.; Sindhu, R.; Patel, A.K.; Binod, P.; et al. Production and Beneficial Impact of Biochar for Environmental Application: A Comprehensive Review. *Bioresour. Technol.* **2021**, *337*, 125451. [CrossRef] [PubMed]
5. Lee, Y.; Park, J.; Ryu, C.; Gang, K.S.; Yang, W.; Park, Y.-K.; Jung, J.; Hyun, S. Comparison of Biochar Properties from Biomass Residues Produced by Slow Pyrolysis at 500 °C. *Bioresour. Technol.* **2013**, *148*, 196–201. [CrossRef] [PubMed]
6. Sachdeva, S.; Kumar, R.; Sahoo, P.K.; Nadda, A.K. Recent Advances in Biochar Amendments for Immobilization of Heavy Metals in an Agricultural Ecosystem: A Systematic Review. *Environ. Pollut.* **2023**, *319*, 120937. [CrossRef]
7. Wang, Y.; Li, H.; Lin, S. Advances in the Study of Heavy Metal Adsorption from Water and Soil by Modified Biochar. *Water* **2022**, *14*, 3894. [CrossRef]

8. Gogoi, L.; Narzari, R.; Chutia, R.S.; Borkotoki, B.; Gogoi, N.; Kataki, R. Chapter Two—Remediation of Heavy Metal Contaminated Soil: Role of Biochar. In *Advances in Chemical Pollution, Environmental Management and Protection*; Sarmah, A.K., Ed.; Biochar: Fundamentals and Applications in Environmental Science and Remediation Technologies; Elsevier: Amsterdam, The Netherlands, 2021; Volume 7, pp. 39–63. [CrossRef]
9. Liang, M.; Lu, L.; He, H.; Li, J.; Zhu, Z.; Zhu, Y. Applications of Biochar and Modified Biochar in Heavy Metal Contaminated Soil: A Descriptive Review. *Sustainability* **2021**, *13*, 14041. [CrossRef]
10. Cheng, S.; Chen, T.; Xu, W.; Huang, J.; Jiang, S.; Yan, B. Application Research of Biochar for the Remediation of Soil Heavy Metals Contamination: A Review. *Molecules* **2020**, *25*, 3167. [CrossRef]
11. Xu, R.; Zhao, A. Effect of Biochars on Adsorption of Cu(II), Pb(II) and Cd(II) by Three Variable Charge Soils from Southern China. *Environ. Sci. Pollut. Res.* **2013**, *20*, 8491–8501. [CrossRef]
12. He, L.; Zhong, H.; Liu, G.; Dai, Z.; Brookes, P.C.; Xu, J. Remediation of Heavy Metal Contaminated Soils by Biochar: Mechanisms, Potential Risks and Applications in China. *Environ. Pollut.* **2019**, *252*, 846–855. [CrossRef] [PubMed]
13. Nkoh, J.N.; Ajibade, F.O.; Atakpa, E.O.; Baquy, M.A.-A.; Mia, S.; Odii, E.C.; Xu, R. Reduction of Heavy Metal Uptake from Polluted Soils and Associated Health Risks Through Biochar Amendment: A Critical Synthesis. *J. Hazard. Mater. Adv.* **2022**, *6*, 100086. [CrossRef]
14. Liang, J.; Li, X.; Yu, Z.; Zeng, G.; Luo, Y.; Jiang, L.; Yang, Z.; Qian, Y.; Wu, H. Amorphous MnO_2 Modified Biochar Derived from Aerobically Composted Swine Manure for Adsorption of Pb(II) and Cd(II). *ACS Sustain. Chem. Eng.* **2017**, *5*, 5049–5058. [CrossRef]
15. Chen, M.; Bao, C.; Hu, D.; Jin, X.; Huang, Q. Facile and Low-Cost Fabrication of ZnO/Biochar Nanocomposites from Jute Fibers for Efficient and Stable Photodegradation of Methylene Blue Dye. *J. Anal. Appl. Pyrolysis* **2019**, *139*, 319–332. [CrossRef]
16. Liu, J.; Jiang, J.; Meng, Y.; Aihemaiti, A.; Xu, Y.; Xiang, H.; Gao, Y.; Chen, X. Preparation, Environmental Application and Prospect of Biochar-Supported Metal Nanoparticles: A Review. *J. Hazard. Mater.* **2020**, *388*, 122026. [CrossRef]
17. Zhao, C.; Wang, B.; Theng, B.K.G.; Wu, P.; Liu, F.; Wang, S.; Lee, X.; Chen, M.; Li, L.; Zhang, X. Formation and Mechanisms of Nano-Metal Oxide-Biochar Composites for Pollutants Removal: A Review. *Sci. Total Environ.* **2021**, *767*, 145305. [CrossRef] [PubMed]
18. Karpuraranjith, M.; Chen, Y.; Ramadoss, M.; Wang, B.; Yang, H.; Rajaboopathi, S.; Yang, D. Magnetically Recyclable Magnetic Biochar Graphitic Carbon Nitride Nanoarchitectures for Highly Efficient Charge Separation and Stable Photocatalytic Activity Under Visible-Light Irradiation. *J. Mol. Liq.* **2021**, *326*, 115315. [CrossRef]
19. Ahuja, R.; Kalia, A.; Sikka, R.; Chaitra, P. Nano Modifications of Biochar to Enhance Heavy Metal Adsorption from Wastewaters: A Review. *ACS Omega* **2022**, *7*, 45825–45836. [CrossRef]
20. Jin, H.; Capareda, S.; Chang, Z.; Gao, J.; Xu, Y.; Zhang, J. Biochar Pyrolytically Produced from Municipal Solid Wastes for Aqueous As(V) Removal: Adsorption Property and Its Improvement with KOH Activation. *Bioresour. Technol.* **2014**, *169*, 622–629. [CrossRef]
21. Mian, M.M.; Liu, G.; Yousaf, B.; Fu, B.; Ullah, H.; Ali, M.U.; Abbas, Q.; Mujtaba Munir, M.A.; Ruijia, L. Simultaneous Functionalization and Magnetization of Biochar Via NH_3 Ambiance Pyrolysis for Efficient Removal of Cr (VI). *Chemosphere* **2018**, *208*, 712–721. [CrossRef]
22. Xue, Y.; Gao, B.; Yao, Y.; Inyang, M.; Zhang, M.; Zimmerman, A.R.; Ro, K.S. Hydrogen Peroxide Modification Enhances the Ability of Biochar (Hydrochar) Produced from Hydrothermal Carbonization of Peanut Hull to Remove Aqueous Heavy Metals: Batch and Column Tests. *Chem. Eng. J.* **2012**, *200–202*, 673–680. [CrossRef]
23. Zhou, Y.; Gao, B.; Zimmerman, A.R.; Fang, J.; Sun, Y.; Cao, X. Sorption of Heavy Metals on Chitosan-Modified Biochars and Its Biological Effects. *Chem. Eng. J.* **2013**, *231*, 512–518. [CrossRef]
24. Fan, J.; Cai, C.; Chi, H.; Reid, B.J.; Coulon, F.; Zhang, Y.; Hou, Y. Remediation of Cadmium and Lead Polluted Soil Using Thiol-Modified Biochar. *J. Hazard. Mater.* **2020**, *388*, 122037. [CrossRef]
25. Liu, Z.; Xu, Z.; Xu, L.; Buyong, F.; Chay, T.C.; Li, Z.; Cai, Y.; Hu, B.; Zhu, Y.; Wang, X. Modified Biochar: Synthesis and Mechanism for Removal of Environmental Heavy Metals. *Carbon Res.* **2022**, *1*, 8. [CrossRef]
26. Huang, Y.; Huang, Y.; Fang, L.; Zhao, B.; Zhang, Y.; Zhu, Y.; Wang, Z.; Wang, Q.; Li, F. Interfacial Chemistry of Mercury on Thiol-Modified Biochar and Its Implication for Adsorbent Engineering. *Chem. Eng. J.* **2023**, *454*, 140310. [CrossRef]
27. Ul Hasan, I.M.; Niazi, N.K.; Bibi, I.; Younas, F.; Al-Misned, F.; Shakoor, M.B.; Ali, F.; Ilyas, S.; Hussain, M.M.; Qiao, J.; et al. Enhanced Capacity of Thiol-Functionalized Sugarcane Bagasse and Rice Husk Biochars for Arsenite Sorption in Aqueous Solutions. *Environ. Sci. Pollut. Res.* **2024**, *31*, 52293–52305. [CrossRef]
28. Jiao, Z.-Q.; Ge, S.-J.; Zheng, W.-X.; Liu, J.-H.; Chen, M.; Kong, Y.-K.; Wang, Y.-Y. Stabilization of Cd-contaminated Soil with Thiol-modified Biochar and Response of Soil Microorganisms. *Huan Jing Ke Xue* **2024**, *45*, 5570–5577. [CrossRef]
29. Wang, Z.; Jia, J.; Liu, W.; Huang, S.; Chen, X.; Zhang, N.; Huang, Y. Mercury Speciation Transformation Mediated by Thiolated Biochar in High Salinity Groundwater: Interfacial Processes, Influencing Factors, and Mechanisms. *Chem. Eng. J.* **2024**, *484*, 149443. [CrossRef]

30. Wang, F.; Jin, L.; Guo, C.; Min, L.; Zhang, P.; Sun, H.; Zhu, H.; Zhang, C. Enhanced Heavy Metals Sorption by Modified Biochars Derived from Pig Manure. *Sci. Total Environ.* **2021**, *786*, 147595. [CrossRef]
31. Lyu, H.; Xia, S.; Tang, J.; Zhang, Y.; Gao, B.; Shen, B. Thiol-Modified Biochar Synthesized by a Facile Ball-Milling Method for Enhanced Sorption of Inorganic Hg^{2+} and Organic CH_3Hg^+. *J. Hazard. Mater.* **2020**, *384*, 121357. [CrossRef]
32. Zhao, L.; Zhang, Y.; Wang, L.; Lyu, H.; Xia, S.; Tang, J. Effective Removal of Hg(II) and MeHg from Aqueous Environment by Ball Milling Aided Thiol-Modification of Biochars: Effect of Different Pyrolysis Temperatures. *Chemosphere* **2022**, *294*, 133820. [CrossRef] [PubMed]
33. Xia, S.; Huang, Y.; Tang, J.; Wang, L. Preparation of Various Thiol-Functionalized Carbon-Based Materials for Enhanced Removal of Mercury from Aqueous Solution. *Environ. Sci. Pollut. Res.* **2019**, *26*, 8709–8720. [CrossRef] [PubMed]
34. Gomez-Marroquín, M.C.; Carbonel, D.; Esquivel, S.; Colorado, H. Thiol-Modified Olive-Stone Biochar Preparation for Hg(II) Removal from Aqueous Solutions. *J. Environ. Eng. Sci.* **2024**, *19*, 177–188. [CrossRef]
35. Fairley, N.; Fernandez, V.; Richard-Plouet, M.; Guillot-Deudon, C.; Walton, J.; Smith, E.; Flahaut, D.; Greiner, M.; Biesinger, M.; Tougaard, S.; et al. Systematic and collaborative approach to problem solving using X-ray photoelectron spectroscopy. *Appl. Surf. Sci. Adv.* **2021**, *5*, 100112. [CrossRef]
36. Huang, Y.; Xia, S.; Lyu, J.; Tang, J. Highly Efficient Removal of Aqueous Hg^{2+} and CH_3Hg^+ by Selective Modification of Biochar with 3-Mercaptopropyltrimethoxysilane. *Chem. Eng. J.* **2019**, *360*, 1646–1655. [CrossRef]
37. Huang, Y.; Tang, J.; Gai, L.; Gong, Y.; Guan, H.; He, R.; Lyu, H. Different Approaches for Preparing a Novel Thiol-Functionalized Graphene Oxide/Fe-Mn and Its Application for Aqueous Methylmercury Removal. *Chem. Eng. J.* **2017**, *319*, 229–239. [CrossRef]
38. Krishna Kumar, A.S.; Jiang, S.-J.; Tseng, W.-L. Facile Synthesis and Characterization of Thiol-Functionalized Graphene Oxide as Effective Adsorbent for Hg(II). *J. Environ. Chem. Eng.* **2016**, *4*, 2052–2065. [CrossRef]
39. Kokkinos, E.; Lampou, A.; Kellartzis, I.; Karfaridis, D.; Zouboulis, A. Thiol-Functionalization Carbonaceous Adsorbents for the Removal of Methyl-Mercury from Water in the ppb Levels. *Water* **2022**, *14*, 49. [CrossRef]
40. Janu, R.; Mrlik, V.; Ribitsch, D.; Hofman, J.; Sedláček, P.; Bielská, L.; Soja, G. Biochar Surface Functional Groups as Affected by Biomass Feedstock, Biochar Composition and Pyrolysis Temperature. *Carbon Resour. Convers.* **2021**, *4*, 36–46. [CrossRef]
41. Chai, L.; Li, Q.; Zhu, Y.; Zhang, Z.; Wang, Q.; Wang, Y.; Yang, Z. Synthesis of Thiol-Functionalized Spent Grain as a Novel Adsorbent for Divalent Metal Ions. *Bioresour. Technol.* **2010**, *101*, 6269–6272. [CrossRef]
42. Matuana, L.M.; Balatinecz, J.J.; Sodhi, R.N.S.; Park, C.B. Surface Characterization of Esterified Cellulosic Fibers by XPS and FTIR Spectroscopy. *Wood Sci. Technol.* **2001**, *35*, 191–201. [CrossRef]
43. Özgenç, Ö.; Durmaz, S.; Boyaci, I.H.; Eksi-Kocak, H. Determination of Chemical Changes in Heat-Treated Wood Using ATR-FTIR and FT Raman Spectrometry. *Spectrochim. Acta Part A Mol. Biomol. Spectrosc.* **2017**, *171*, 395–400. [CrossRef]
44. Aldana-Pérez, A.; Lartundo-Rojas, L.; Gómez, R.; Niño-Gómez, M.E. Sulfonic Groups Anchored on Mesoporous Carbon Starbons-300 and Its Use for the Esterification of Oleic Acid. *Fuel* **2012**, *100*, 128–138. [CrossRef]
45. Desroches, M.; Caillol, S.; Auvergne, R.; Boutevin, B.; David, G. Biobased Cross-Linked Polyurethanes Obtained from Ester/Amide Pseudo-Diols of Fatty Acid Derivatives Synthesized by Thiol–Ene Coupling. *Polym. Chem.* **2012**, *3*, 450–457. [CrossRef]
46. Huang, Y.; Gong, Y.; Tang, J.; Xia, S. Effective Removal of Inorganic Mercury and Methylmercury from Aqueous Solution Using Novel Thiol-Functionalized Graphene Oxide/Fe-Mn Composite. *J. Hazard. Mater.* **2019**, *366*, 130–139. [CrossRef] [PubMed]
47. Zhu, L.; Lei, H.; Wang, L.; Yadavalli, G.; Zhang, X.; Wei, Y.; Liu, Y.; Yan, D.; Chen, S.; Ahring, B. Biochar of Corn Stover: Microwave-Assisted Pyrolysis Condition Induced Changes in Surface Functional Groups and Characteristics. *J. Anal. Appl. Pyrolysis* **2015**, *115*, 149–156. [CrossRef]
48. Song, S.; Zhang, Y. Construction of a 3D Multiple Network Skeleton by the Thiol-Michael Addition Click Reaction to Fabricate Novel Polymer/Graphene Aerogels with Exceptional Thermal Conductivity and Mechanical Properties. *J. Mater. Chem. A* **2017**, *5*, 22352–22360. [CrossRef]
49. Samal, S.; Geckeler, K.E. Unexpected Solute Aggregation in Water on Dilution. *Chem. Commun.* **2001**, *21*, 2224–2225. [CrossRef]
50. Lyu, H.; Gao, B.; He, F.; Zimmerman, A.R.; Ding, C.; Huang, H.; Tang, J. Effects of Ball Milling on the Physicochemical and Sorptive Properties of Biochar: Experimental Observations and Governing Mechanisms. *Environ. Pollut.* **2018**, *233*, 54–63. [CrossRef]
51. Julien, F.; Baudu, M.; Mazet, M. Relationship Between Chemical and Physical Surface Properties of Activated Carbon. *Water Res.* **1998**, *32*, 3414–3424. [CrossRef]
52. Batista, E.M.C.C.; Shultz, J.; Matos, T.T.S.; Fornari, M.R.; Ferreira, T.M.; Szpoganicz, B.; de Freitas, R.A.; Mangrich, A.S. Effect of Surface and Porosity of Biochar on Water Holding Capacity Aiming Indirectly at Preservation of the Amazon Biome. *Sci. Rep.* **2018**, *8*, 10677. [CrossRef] [PubMed]
53. Peng, Z.; Zhao, H.; Lyu, H.; Wang, L.; Huang, H.; Nan, Q.; Tang, J. UV Modification of Biochar for Enhanced Hexavalent Chromium Removal from Aqueous Solution. *Environ. Sci. Pollut. Res.* **2018**, *25*, 10808–10819. [CrossRef] [PubMed]
54. Liu, Z.; Ling, X.Y.; Guo, B.; Hong, L.; Lee, J.Y. Pt and PtRu Nanoparticles Deposited on Single-Wall Carbon Nanotubes for Methanol Electro-Oxidation. *J. Power Sources* **2007**, *167*, 272–280. [CrossRef]

55. Carriere, B.; Deville, J.P.; Brion, D.; Escard, J. X-Ray Photoelectron Study of Some Silicon-Oxygen Compounds. *J. Electron Spectrosc. Relat. Phenom.* **1977**, *10*, 85–91. [CrossRef]
56. Xu, X.; Zheng, Y.; Gao, B.; Cao, X. N-Doped Biochar Synthesized by a Facile Ball-Milling Method for Enhanced Sorption of CO_2 and Reactive Red. *Chem. Eng. J.* **2019**, *368*, 564–572. [CrossRef]

Disclaimer/Publisher's Note: The statements, opinions and data contained in all publications are solely those of the individual author(s) and contributor(s) and not of MDPI and/or the editor(s). MDPI and/or the editor(s) disclaim responsibility for any injury to people or property resulting from any ideas, methods, instructions or products referred to in the content.